Science Signaling
AAAS

www.sciencesignaling.org/cgi/content/full/3/108/ra9/DC1

Supplementary Materials for

ARD1 Stabilization of TSC2 Suppresses Tumorigenesis Through the mTOR Signaling Pathway

Hsu-Ping Kuo, Dung-Fang Lee, Chun-Te Chen, Mo Liu, Chao-Kai Chou, Hong-Jen Lee, Yi Du, Xiaoming Xie, Yongkun Wei, Weiya Xia, Zhang Weihua, Jer-Yen Yang, Chia-Jui Yen, Tzu-Hsuan Huang, Minjia Tan, Gang Xing, Yingming Zhao, Chien-Hsing Lin, Shih-Feng Tsai, Isaiah J. Fidler, Mien-Chie Hung*

*To whom correspondence should be addressed. E-mail: mhung@mdanderson.org

Published 9 February 2010, *Sci. Signal.* **3**, ra9 (2010)
DOI: 10.1126/scisignal.2000590

This PDF file includes:

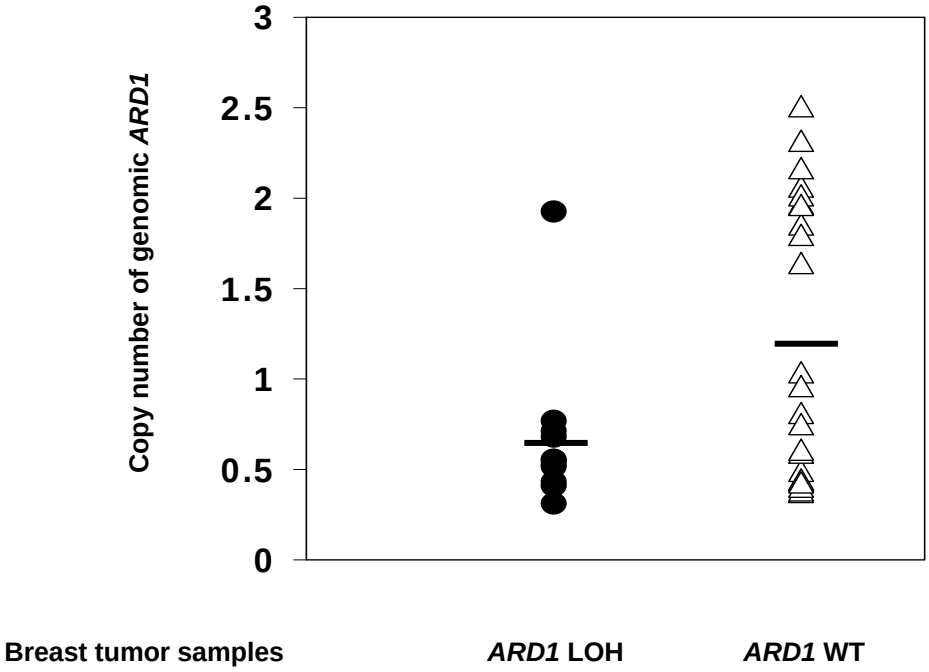

Fig. S1. Lower copy number of genomic *ARD1* was found in *ARD1* LOH group compared to that in *ARD1* wild-type (WT) group ($P<0.05$; *t* test). The graph shows the relative copy number of genomic *ARD1* that is standardized to 1 for the normal breast cell line MCF-10A sample, and the lines indicate the average of relative copy number of both groups.

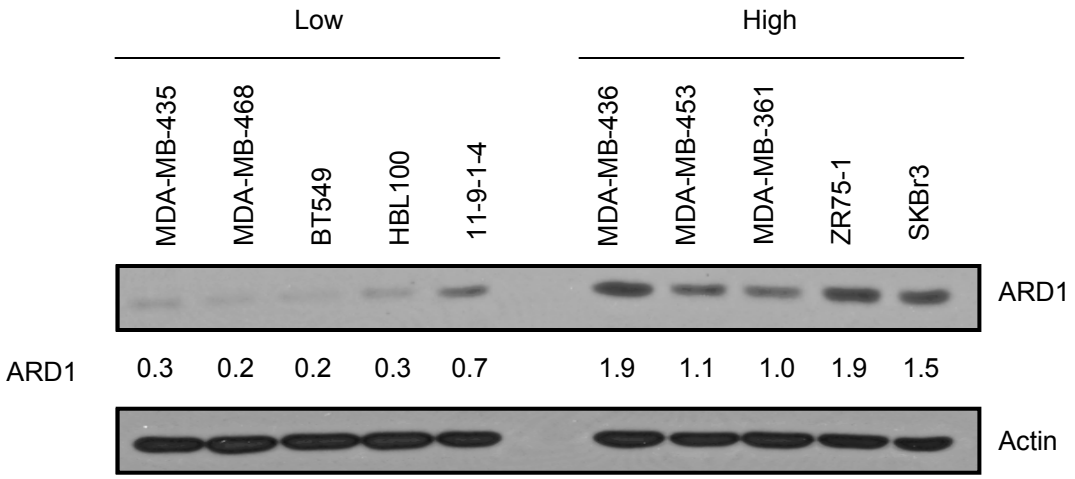

Fig. S2. Endogenous ARD1 in five cell lines with low ARD1 abundance (MDA-MB-435, MDA-MB-468, BT549, HBL100, 11-9-1-4) and five cell lines with high ARD1 abundance (MDA-MB-436, MDA-MB-453, MDA-MB-361, ZR75-1, SKBr3).

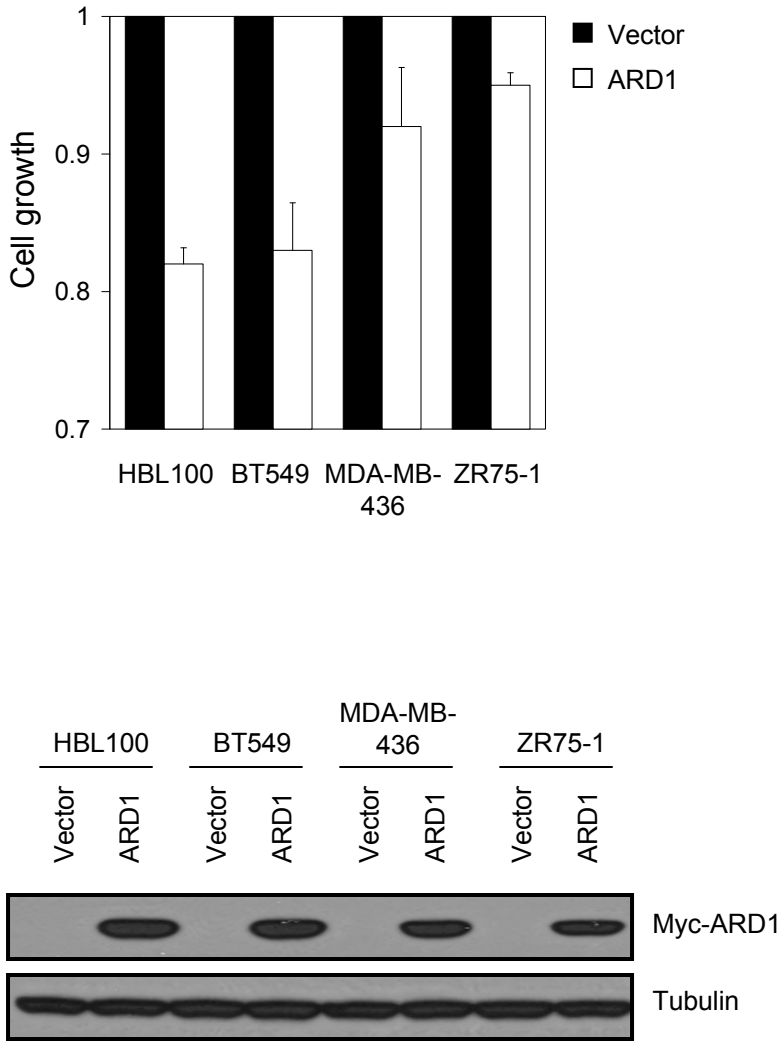

Fig. S3. Myc-ARD1 had a stronger growth-inhibitory effect in tumor cells with lower endogenous ARD1 (HBL100 and BT549) than in cells with abundant endogenous ARD1 (MDA-MB-436 and ZR75-1) ($P<0.05$; *t* test). Error bars represent SD (n = 5).

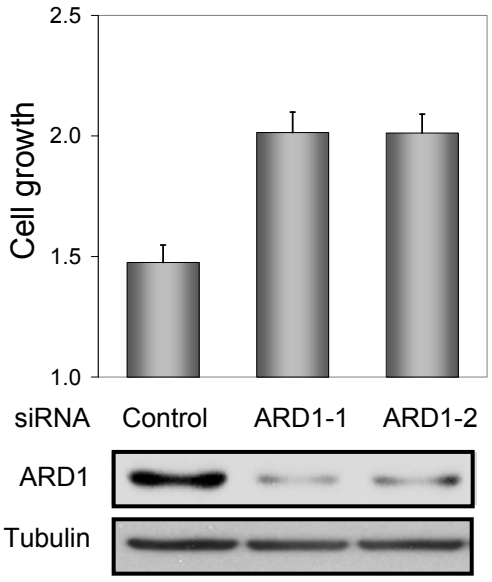

Fig. S4. Knockdown of ARD1 with either of two different siRNAs increased the growth of MDA-MB-435 cells ($P<0.05$; *t* test). The cell growth rate was analyzed by an MTT assay. Error bars represent SD (n = 5).

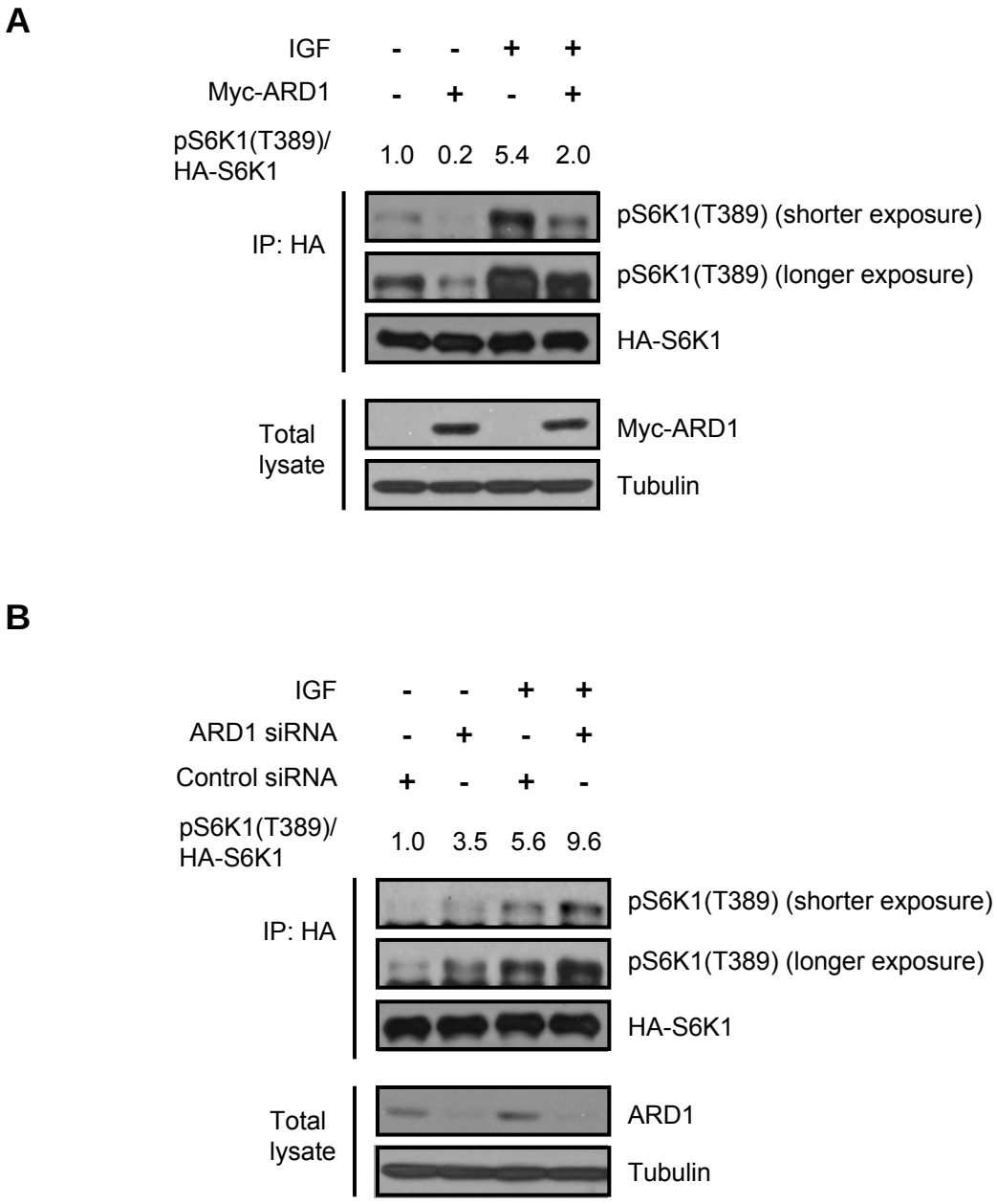

Fig. S5. ARD1 reduced the degree of pS6K1(T389) **(A)** whereas depletion of ARD1 increased pS6K1(T389) **(B)** under conditions of both serum starvation and insulin-like growth factor (IGF) stimulation. HEK293T cells were serum-starved overnight and then treated with 20 ng/ml IGF for 30 min.

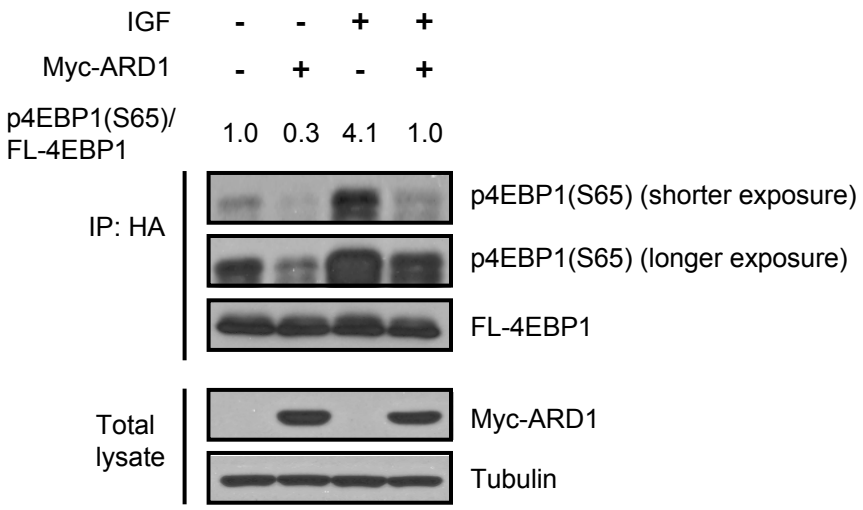

Fig. S6. ARD1 reduced p4EBP1(S65) under conditions of both serum starvation and IGF stimulation. HEK293T cells were serum-starved overnight and then treated with 20 ng/ml IGF for 30 min.

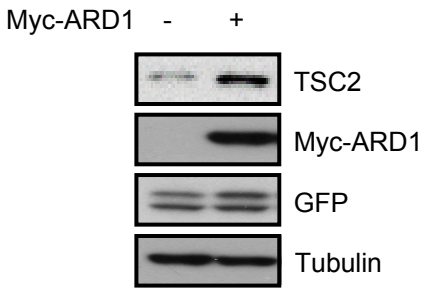

Fig. S7. Transient transfection of Myc-ARD1 increased the amount of TSC2 in HEK293T cells.

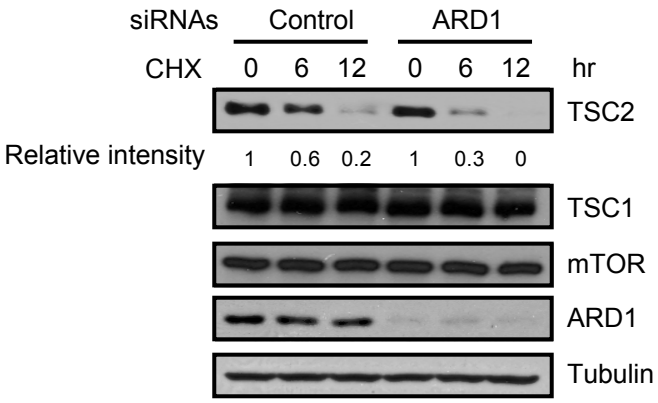

Fig. S8. Depletion of ARD1 decreased the stability of TSC2. The relative intensity of TSC2 was standardized to 1 for the cycloheximide-pretreated (CHX 0 hours) sample.

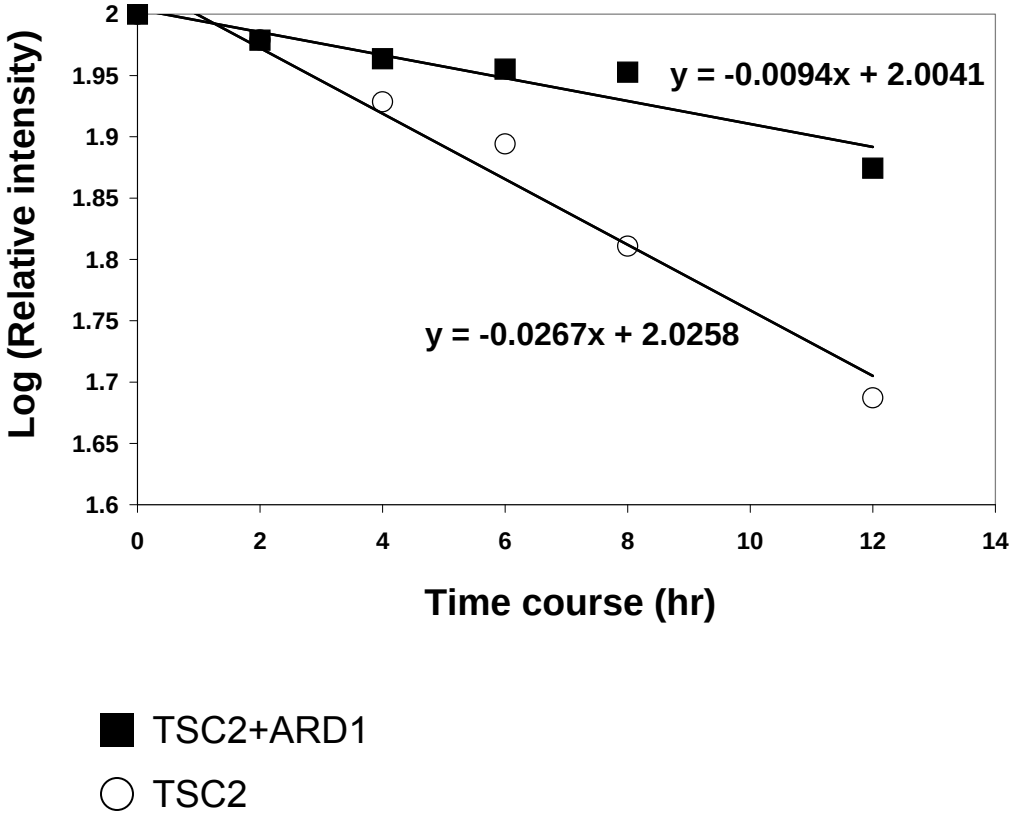

Fig. S9. The data of Fig. 6B on a semilog plot.

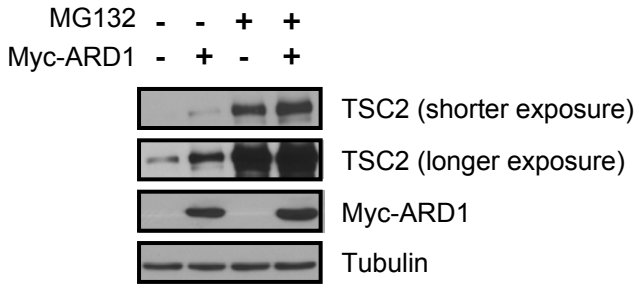

Fig. S10. Treatment of MG132 increased TSC2 abundance. MG132 was added to HEK293T cells 6 hours before they were harvested for analysis.

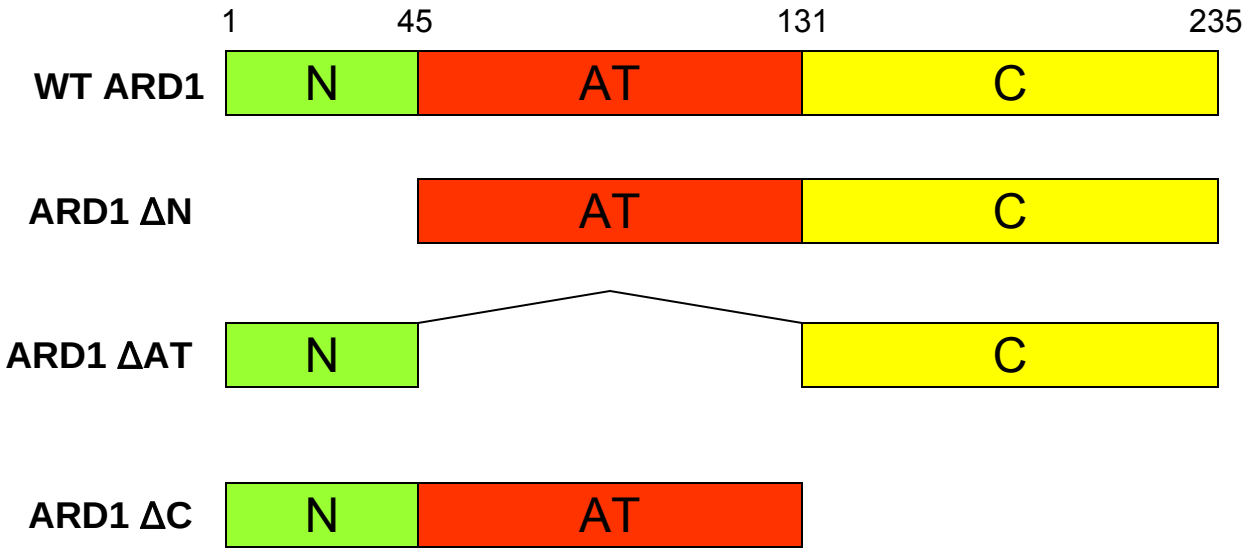

Fig. S11. Schematic shows wild-type (WT) ARD1 and three truncated forms of ARD1, including ARD1 ΔN (deletion of N-terminal domain (amino acids 1-44)), ARD1 ΔAT (deletion of acetyltransferase domain (amino acids 45-130)), and ARD1 ΔC (deletion of C-terminal domain (amino acids 131-235)).

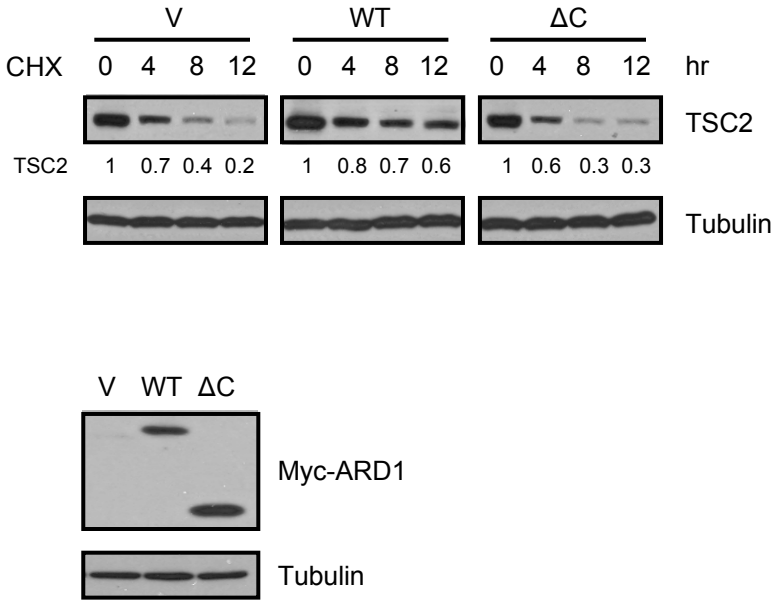

Fig. S12. WT ARD1, but not ARD1 ΔC, increased the stability of TSC2.

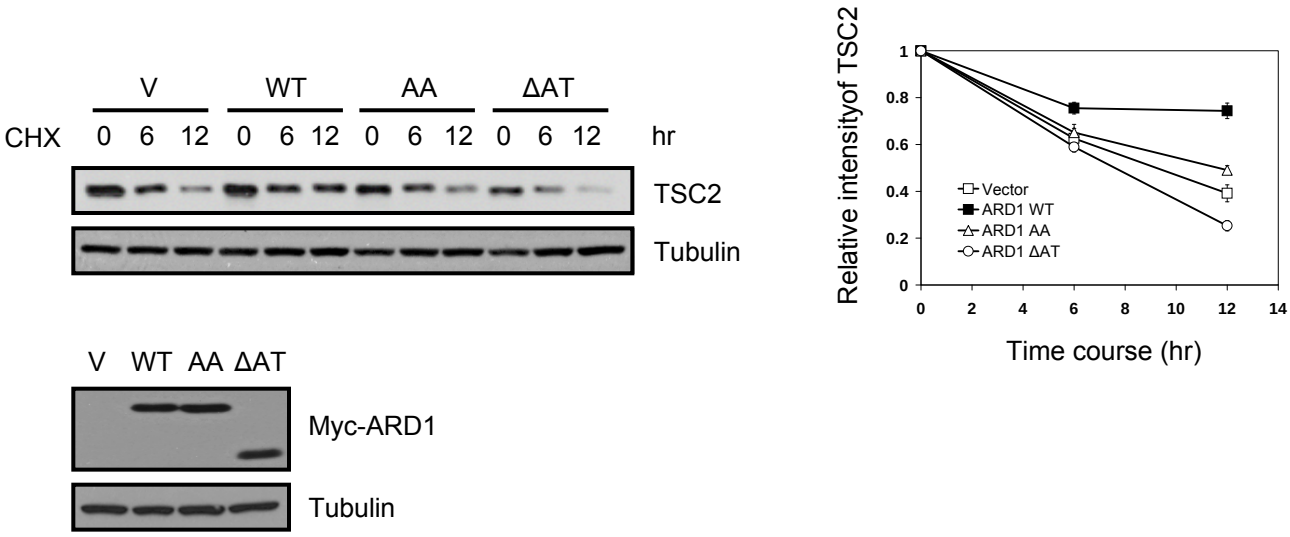

Fig. S13. WT ARD1, but not ARD1 AA or ARD1 ΔAT, stabilized TSC2. The graph shows the relative intensity of TSC2 at different time points after cycloheximide treatment standardized to 1 for the cycloheximide-pretreated (CHX 0 hours) sample for vector control or each of the ARD1 constructs. Error bars represent SD (n = 3).

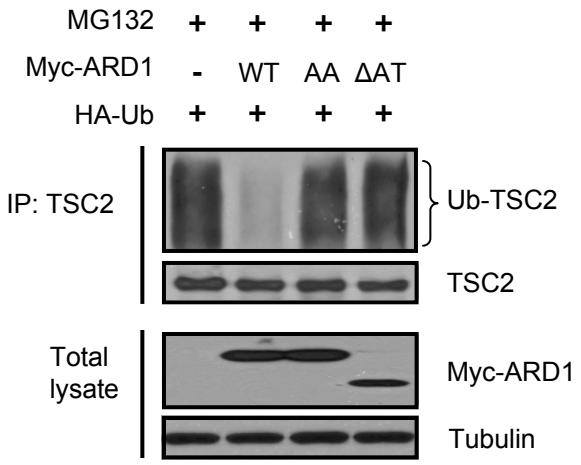

Fig. S14. WT ARD1, but not ARD1 AA or ARD1 ΔAT, reduced ubiquitination of TSC2.

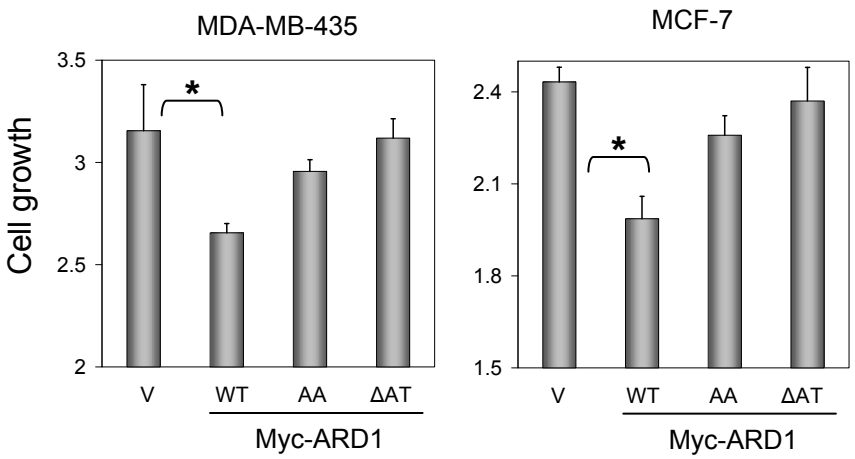

Fig. S15. WT ARD1, but not ARD1 AA or ARD1 ΔAT, significantly suppressed the growth of MDA-MB-435 and MCF-7 cells (*, $P<0.05$; *t* test). Error bars represent SD (n = 5).

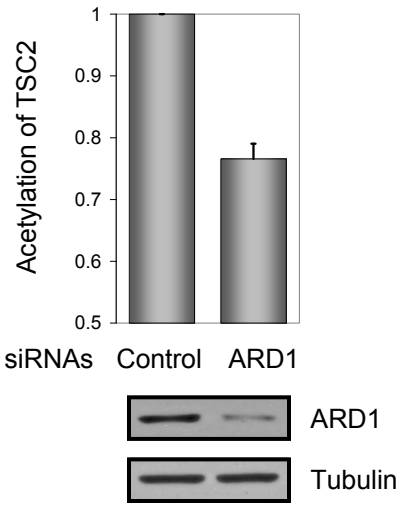

Fig. S16. Depletion of ARD1 decreased the acetylation of endogenous TSC2. Forty-eight hours after ARD1 knockdown, cells were labeled with 1 mCi/ml [^{3}H]-sodium acetate for 3 hours. TSC2 immunoprecipitates were then purified and radioactivity was measured by scintillation counting. Error bars represent SD (n = 3).

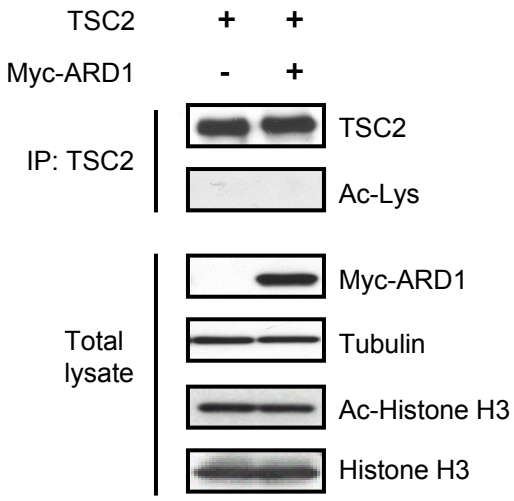

Fig. S17. We detected no ARD1-induced ε-acetylation of TSC2.

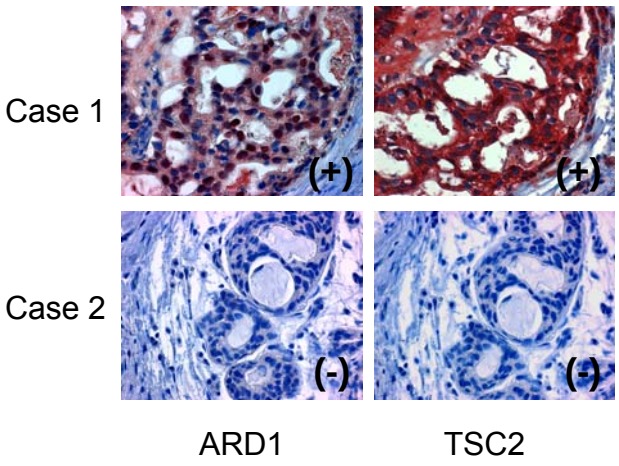

Fig. S18. Shown are two representative breast cancer specimens with consecutive sections. Immunoreaction with red color indicates ARD1/TSC2 protein expression. Positive staining for ARD1 and TSC2 was shown in the specimens of case 1 while negative staining for ARD1 and TSC2 was shown in the specimens of case 2.

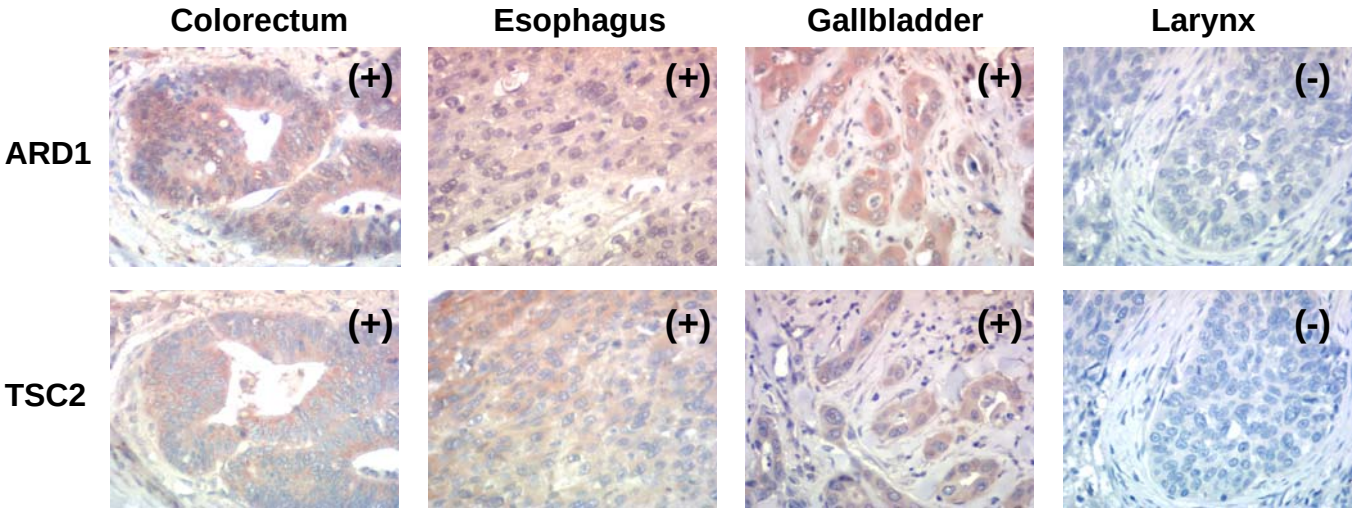

Fig. S19. Representative images of ARD1 and TSC2 abundance in four different types of cancers.

Supplemental Table 1

Relationship between ARD1 and TSC2 in surgical specimens of various tumors

Organ	No. of Specimens	No. of ARD1 (-)	No. of ARD1 (+)	No. of ARD1 (++)	No. of ARD1 (+++)	No. of TSC2 (-)	No. of TSC2 (+)	No. of TSC2 (++)	No. of TSC2 (+++)
Oral cavity	5	2	1	1	1	2	2	1	0
Nasopharynx	4	0	3	1	0	1	2	1	0
Salivary gland	9	2	4	2	1	3	6	0	0
Esophagus	3	1	0	1	1	1	0	1	1
Stomach	23	7	3	9	4	9	6	4	4
Small intestine	4	3	0	1	0	3	1	0	0
Colorectum	27	8	7	7	5	14	6	1	6
Liver	14	8	1	4	1	11	1	1	1
Gallbladder	5	4	1	0	0	4	1	0	0
Pancreas	3	0	1	2	0	2	0	0	1
Larynx	13	9	3	1	0	9	3	0	1
Lung	7	5	0	1	1	7	0	0	0
Total	117	49	24	30	14	66	28	9	14